

Polariton modes and materials parameters in Li_2GeO_3

Y. S. Yu,* S. S. Prabhu, and S. Perkowitz

Physics Department, Emory University, Atlanta, Georgia 30322-2430

S. C. Kim

Physics Department, Dongeui University, 614-714 Pusan, Korea

(Received 10 March 1997)

We have observed polariton modes in Li_2GeO_3 , and measured their dispersion curves by Raman scattering in the near-forward-angle geometry. We determined the low-frequency dielectric constant $\epsilon(0)$ by making a theoretical fit to the dispersion curve for a low-frequency polariton, and also by using our measured values of transverse-optical and longitudinal-optical mode frequencies in the extended Lyddane-Sachs-Teller relationship. The two approaches yield $\epsilon(0) = 15.0 \pm 0.3$, a value that we compare to results from infrared data and in the near-dc limit. [S0163-1829(97)03834-4]

I. INTRODUCTION

Li_2GeO_3 is an interesting material because of the complexity of its phonon modes, and because it has potential for use in acousto-optic, piezoelectric, and pyroelectric devices. In such a polar crystal, the transverse-optical (TO) phonons interact strongly with infrared radiation. Hopfield¹ has proposed a general theory for these mixed mechanical and electromagnetic excitations, which he called polaritons. Henry and Hopfield² observed a polariton in Raman scattering from cubic GaP, and Porto, Tell, and Damen³ studied polaritons in hexagonal ZnO. GaP and ZnO are simple crystals with diatomic lattice structure and a single TO phonon. In crystals with two or more TO modes, polaritons become far more complex. Scott⁴ measured three dispersive polariton modes in α -quartz, which has nine atoms per unit cell and eight TO phonons of symmetry type E . Since then, polaritons have been observed in Raman scattering from various crystals with complex structures.^{5,6}

In this study, we examine polariton modes with $A_1(z)$ symmetry in single crystal Li_2GeO_3 by means of Raman scattering, and determine their dispersion curves, wave number vs frequency, by careful measurements of Raman frequency vs angle of incidence of the incoming light. We fit the measured dispersion curve with polariton theory, which yields the low-frequency dielectric constant $\epsilon(0)$ for Li_2GeO_3 . We obtain a second value of $\epsilon(0)$ from the generalized Lyddane-Sachs-Teller (LST) relation,⁷ which uses our measured values for all the transverse-optical (TO) and longitudinal-optical (LO) mode frequencies: and a third value from infrared reflectivity data. The dielectric constants obtained from these methods are similar, and comparable with the near-dc value.⁸ Our results further elucidate polariton modes in complex crystals, and show how their Raman analysis can give $\epsilon(0)$ as well as the TO and LO frequencies, important materials parameters for Li_2GeO_3 .

II. DISCUSSION AND RESULTS

The dispersion relation for a polariton is determined from its dielectric function $\epsilon(\omega)$, which for a multipolariton system is given by⁹

$$\epsilon(\omega) = \epsilon(\infty) + \sum S_i \omega_{Ti}^2 (\omega_{Ti}^2 - \omega^2)^{-1} \quad (1)$$

where the sum is over N vibrational modes; $\epsilon(\infty)$ is the high-frequency dielectric constant of the crystal; S_i and ω_{Ti} are the dimensionless mode strength, and resonant frequency, respectively, of the i th normal TO mode. Lattice damping has been ignored in Eq. (1), which is not a serious deficiency in the model. In the limit $\omega \rightarrow 0$, this expression gives the low-frequency dielectric constant as

$$\epsilon(0) = \epsilon(\infty) + \sum S_i. \quad (2)$$

The dispersion relation for the polariton is given by the definition

$$q^2 = \frac{\omega^2}{c^2} \epsilon(\omega), \quad (3)$$

where q is the wave vector, ω is the angular frequency, and c is the velocity of light. In the low-frequency limit, this gives a simple linear relation between q and ω , namely

$$q = \frac{\omega}{c} \sqrt{\epsilon(0)}, \quad (4)$$

so that $\epsilon(0)$ can be obtained from the slope of the dispersion curve as $\omega \rightarrow 0$. However, in this paper we employ a more definitive method: we fit our measured dispersion curve over a range of frequency with Eq. (1).

Another expression relevant to our determination of $\epsilon(0)$ is the Lyddane-Sachs-Teller (LST) relation derived by Lyddane, Sachs, and Teller¹⁰ for a single undamped vibrational mode. That result has been extended into a generalized LST relation for multiple modes through a specific model employed by Kurosawa¹¹ and Cochran and Cowley,¹² which yields

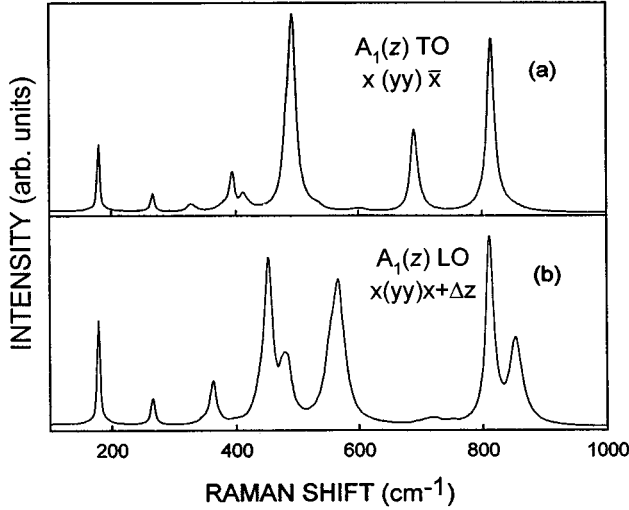


FIG. 1. Raman spectra in the $A_1(z)$ scattering geometry. (a) $A_1(z)$ TO Raman spectrum. (b) $A_1(z)$ LO Raman spectrum.

$$\frac{\varepsilon(0)}{\varepsilon(\infty)} = \prod \frac{\omega_{Li}^2}{\omega_{Ti}^2} \quad (5)$$

where ω_{Ti} and ω_{Li} are the transverse and longitudinal frequencies, respectively, for the i th mode. The product is taken over all the polar modes along one of the axes in the crystal.

A third way to determine $\varepsilon(0)$ comes from the measurement of infrared reflectivity as $\omega \rightarrow 0$: in practice, that means at frequencies much lower than the lowest TO frequency in Eq. (1). At normal incidence, the measured reflection coefficient R is related to the low-frequency refractive index n by the relation

$$R = \frac{(n-1)^2}{(n+1)^2} \quad (6)$$

and $\varepsilon(0)$ is given by n^2 .

Our single-crystal sample of Li_2GeO_3 was grown in air by the Czochralski method. Li_2GeO_3 is an orthorhombic crystal with the C_{2v} ($mm2$) point group. It has two Li_2GeO_3 molecules per primitive cell. Its vibrational modes, as calculated by group theory, are $10A_1(z) + 8A_2 + 8B_1(x) + 10B_2(y)$. Subtracting three acoustic modes gives the 33 optical vibrational modes $9A_1(z) + 8A_2 + 7B_1(x) + 9B_2(y)$, which are all Raman active. Figure 1 shows our Raman data, obtained in the back and near-forward-scattering geometries, for the nine TO and LO modes of the $A_1(z)$ type. Their frequencies appear in Table I.

TABLE I. Frequencies of the $A_1(z)$ TO and LO modes in Li_2GeO_3 from Raman scattering. The backward and near-forward-scattering geometries are used to obtain the TO and the LO modes, respectively.

| | Mode frequencies (cm^{-1}) | | | | | | | | |
|----|---------------------------------------|-----|-----|-----|-----|-----|-----|-----|-----|
| TO | 178 | 267 | 330 | 396 | 413 | 486 | 496 | 697 | 818 |
| LO | 179 | 268 | 364 | 455 | 483 | 555 | 569 | 807 | 840 |

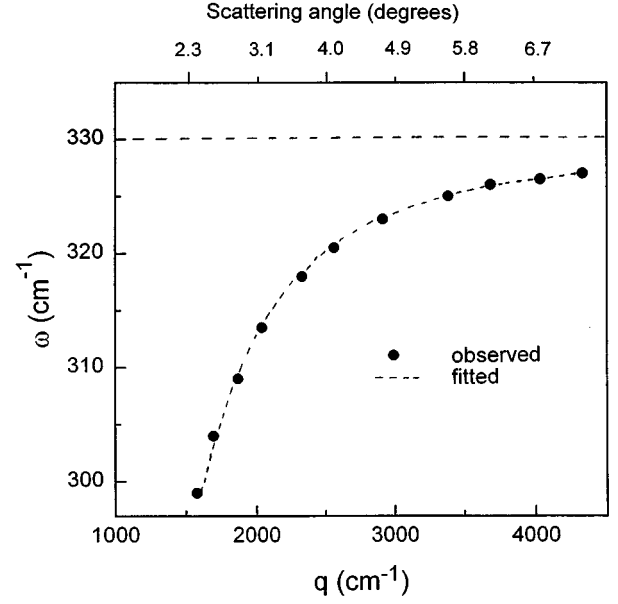


FIG. 2. Measured and fitted polariton frequencies vs wave vector for the $A_1(z)$ TO mode at 330 cm^{-1} .

To determine polariton dispersion, we used the fact that the wave vector q depends on the scattering angle θ between the incident light, and the scattered light inside the crystal, according to the expression that represents conservation of photon momentum

$$q^2 = k_L^2 + k_S^2 - 2k_L k_S \cos \theta, \quad (7)$$

where k_L and k_S are the wave vector of the incident and the Stokes-scattered light, respectively. Hence, by varying θ , q can be swept through a range of values. To set and control θ , we remove the direct beam by using a beam stop with a hole oriented along the direction of the crystal b axis. For $\theta < 2.5^\circ$, we vary the angle by moving the hole along the b axis; for $\theta > 2.5^\circ$, we vary it by changing the distance from the hole to the crystal. This method allows us to measure the angle with high precision, giving a typical accuracy of 0.1° in the value of θ that we use in Eq. (7).

We measured q vs ω for all five $A_1(z)$ polariton modes we observed that showed significant dispersion. In Fig. 2 we display the clearest dispersion curve appearing for a low-frequency polariton, the $A_1(z)$ TO mode at 330 cm^{-1} . We fit this curve using Eqs. (1) and (3). In Eq. (1), we assumed that near 330 cm^{-1} , none of the other eight $A_1(z)$ modes shows significant frequency dependence compared to that from the 330 cm^{-1} mode itself. Hence we approximated the sum of oscillators in Eq. (1) with one oscillator of strength S at 330 cm^{-1} , and an additive constant $C = \varepsilon(\infty) + \Delta\varepsilon$, where $\Delta\varepsilon$ is the constant contribution from the other modes. We varied C and S to yield the excellent least-squares fit to the data shown as the dashed line in the figure, and from this fit obtained $\varepsilon(0) = C + S = 14.8$. Our Raman data yield a second measured result for $\varepsilon(0)$ when we insert the measured TO and LO frequencies, and the value $\varepsilon(\infty) = 2.9$ given by Lurio and Burns,⁸ into Eq. (5). The result is $\varepsilon(0) = 15.2$, which agrees within 2% with the value obtained from the dispersion analysis.

A third value of $\varepsilon(0)$ comes from infrared reflectivity data we obtained with a conventional Fourier transform spectrometer over the range 50–100 cm^{-1} , which give $\varepsilon(0)=13.3$. This lies within 11% of the Raman result, reasonable agreement considering that the infrared reflectivity was not measured to a high degree of accuracy. Our infrared result also agrees with the value 13.6 obtained by Lurio and Burns at 10 kHz, that is, in the near-dc limit. However, the result $\varepsilon(0)=7.6$ that Lurio and Burns report from their infrared reflectivity data seems not to be valid. We are continuing to examine polaritons of other symmetries in Li_2GeO_3 , to

elucidate their behavior and to further explore the properties of this material.

ACKNOWLEDGMENTS

We thank Emory University for its support of this work through its Central Raman Scattering Facility. Y.S.Y. and S.C.K. wish to thank Dongeui University and the Korea Science and Engineering Foundation (KOSEF) through the Science Research Center (SRC) for their support.

*Permanent address: Physics Department, Dongeui University, 614-714 Pusan, Korea.

¹J. J. Hopfield, Phys. Rev. **112**, 1555 (1958).

²C. H. Henry and J. J. Hopfield, Phys. Rev. Lett. **15**, 964 (1965).

³S. P. S. Porto, B. Tell, and T. C. Damen, Phys. Rev. Lett. **16**, 450 (1966).

⁴J. F. Scott, L. E. Cheesman, and S. P. S. Porto, Phys. Rev. **162**, 834 (1967).

⁵T. Fukumoto, A. Okamoto, T. Hattori, and A. Mitsuishi, Solid State Commun. **17**, 427 (1975).

⁶Gary P. Wiederrecht, Thomas P. Dougherty, Lisa Dhar, and Keith

A. Nelson, Ferroelectrics **150**, 103 (1993).

⁷A. S. Barker, Jr., Phys. Rev. B **12**, 4071 (1975).

⁸A. Lurio and G. Burns, Phys. Rev. B **10**, 3512 (1974).

⁹C. M. Hartwig, D. L. Rousseau, and S. P. S. Porto, Phys. Rev. **188**, 1328 (1969).

¹⁰R. H. Lyddane, R. G. Sachs, and E. Teller, Phys. Rev. **59**, 673 (1941).

¹¹T. Kurosawa, J. Phys. Soc. Jpn. **16**, 1298 (1961).

¹²W. Cochran and R. A. Cowley, J. Phys. Chem. Solids **23**, 447 (1962).